AIAA SciTech Forum
6-10 January 2020, Orlando, FL
AIAA Scitech 2020 Forum

10.2514/6.2020-0979

Korea Human Powered Aircraft Competition Lessons Learned

Ki Ju Kwon* and Hak-Tae Lee†
Inha University, Incheon, Republic of Korea, 22212

This paper describes aircraft design methodologies that were developed to design human powered aircraft for the 2014 and 2015 Korea Human Powered Aircraft Competition and the lessons learned from building and flying the two human powered aircraft. As the main participants of the competitions were undergraduate students who are not experienced with aircraft design and construction, constraints such as skill level, transportation, or other logistical issues became important. Two design methodologies, one aerodynamic and one structural technique were developed to address the problems. For the aerodynamic design, lifting tail was used to minimize the size of the aircraft while providing opportunities to practice building techniques using the horizontal tail. For the structural design, a technique to calculate the stress in the spar caps in the presence of bracing wires are developed using a simple beam theory. During the two-year period, two aircraft were designed and built. The first aircraft flew about 75 meters and demonstrated the effectiveness of the design. The second aircraft employed numerous improvements from the initial experience that resulted in a lighter structure with a larger wingspan. However, the main spar structure failed right after takeoff. The characteristics of each aircraft, flight results, and lessons learned through the whole process are presented in the paper.

I. Nomenclature

$\bar{c}_w$	=	mean aerodynamic chord of the main wing
$\bar{c}_t$	=	mean aerodynamic chord of the tail
l_{ac}	=	distance between the aerodynamic centers of the main wing and the horizontal tail
x_{np}	=	position of the neutral point
x_{cg}	=	position of the center of gravity
y_w	=	wire anchoring position along the spar from the root
z_w	=	vertical location of the wire anchoring point at the fuselage
C_{L_w}	=	lift coefficient of main wing
C_{L_t}	=	lift coefficient of horizontal tail
$C_{L_{aw}}$	=	lift curve slope of main wing
$C_{L_{at}}$	=	lift curve slope of horizontal tail
C_{M_w}	=	pitching moment coefficient of main wing
C_{M_t}	=	pitching moment coefficient of horizontal tail
E	=	Young's modulus
I	=	moment of inertia of the spar
M	=	bending moment
SM	=	static margin
T_w	=	tension of the bracing wire
τ	=	normal stress

II. Introduction

Even though the Daedalus human powered aircraft (HPA) set the world record in 1988 [1], there hasn't been any serious effort to build an HPA in the Republic of Korea. To promote public interest in aviation and to provide undergraduate students with hands-on design and construction experiences, Korea Aerospace Research Institute held

*Ph.D Student, Dept. of Aerospace Engineering, 100 Inha-Ro, Michuhol-gu, Incheon 22212, Republic of Korea.
†Associate Professor, Dept. of Aerospace Engineering, 100 Inha-Ro, Michuhol-gu, Incheon 22212, Republic of Korea, AIAA Member.

HPA competitions from 2013 to 2015. Every year, about ten teams, mostly from the Aerospace Engineering departments in the nation, participated. Students of the Dept. Aerospace Engineering, Inha University, participated in all of those competitions, and their aircraft flew successfully in 2014 and 2015. From the first competition, it was discovered that, in addition to the major constraint of marginally sufficient human power, practical problems such as skill level of the participating students, transportation and handling of the aircraft, or the cost of construction were almost as important as the main aircraft design constraints. To overcome these issues, a decision was made to make the aircraft smaller and simpler at the cost of the aerodynamic performances and structural weight.

The most commonly available cargo truck had a bed length of ten meters. Moreover, the company contracted to manufacture the Carbon Fiber Reinforced Plastic (CFRP) composite spars for the competition provided only tapered tubes, which made it very difficult to join multiple sections. So, the Inha University team decided to build their aircraft with two piece-wing with a total span of around twenty meters, which is generally considered not enough.

To overcome the insufficient wing area, lifting tail design was used for the 2014 and 2015 aircraft. The lifting tail not only provided additional lift but also provided opportunities for the students to practice the construction methods using a smaller wing that is much easier to handle.

Two design methodologies were specifically developed for the HPAs that uses only undergraduate level class knowledge combined with a widely used vortex panel tool, AVL [2]. For the aerodynamics, a method to determine the length between the wing and tail was developed. With the given geometric shapes and lift coefficients of the wing and tail as well as static margin, the distance between the two wings is obtained as a dependent variable. This enabled the aircraft to be trimmed precisely at the high design C_L while having a large static margin, high tail volume, and short fuselage. For structural design, the spars are analyzed using the simplest Euler-Bernoulli beam theory ignoring the shear stress. A methodology to calculate the stress in the presence of bracing wire is developed and used to determine the required wire strength and anchoring position.

The 2014 HPA was designed conservatively with 21 m wingspan and 35 kg empty weight. It successfully flew about 75 meters during the competition. The 2015 HPA was designed more aggressively based upon the data and experience gathered from the previous aircraft. Wingspan was increased to 23 meters and the weight was reduced to 30 kg. However, even though the 2015 HPA was superior to the 2014 model in many ways, it experienced a spar failure during the flight that resulted in shorter flight distance than the 2014 HPA.

Following this introduction, Section III explains the aerodynamic design including the lifting tail design methodology. Section IV explains the structural analysis techniques. Section V describes the two aircraft with the flight results. Lessons learned through participating in the competitions are discuss in Section VI, and Section **??** concludes the paper.

III. Aerodynamic Design

To compensate for the lift deficiency of the smaller main wing, a relatively larger lifting horizontal tail was utilized. The design process is based on [3]. The crux of this design methodology is that the lift coefficients of both the wings as well as the static margin can be arbitrarily specified as independent variables. The distance between the aerodynamic centers of the two wings is then calculated as the dependent variable.

Another benefit of lifting tail design is that the center of gravity (c.g.) is located behind the aerodynamic center of the main wing. This enables the pilot to be located directly below the wing, and the overhang from the leading edge of the main wing to the propeller can be reduced. As shown in Fig. 1, the sprocket can be fully exposed in front of the fuselage boom with a short propeller shaft and the chain drive system located directly beneath the sprocket.

A. Trim condition

Figure 2 shows the relative dimensions of the main wing and tail combination. The position of the neutral point can be expressed using Eq. (1), and if the static margin, SM, is specified, the moment balance around the c.g. is express in Eq. (2).

r_s is the area ratio (S_t/S_w); r_α is the lift curve slope ratio ($C_{L_{t_\alpha}}/C_{L_{w_\alpha}}$); r_c is the chord ratio ($\bar{c}_t/\bar{c}_w$); and r_{C_L} is the lift coefficient ratio (C_{L_t}/C_{L_w}) of the main wing and the horizontal tail. Note that the lift curve slope of the horizontal tail assumes it is under the downwash of the main wing.

$$x_{np} = \frac{r_s r_\alpha l_{ac}}{1 + r_s r_\alpha} \tag{1}$$

Fig. 1 Front part of the fuselage of the 2015 HPA with almost no overhang.

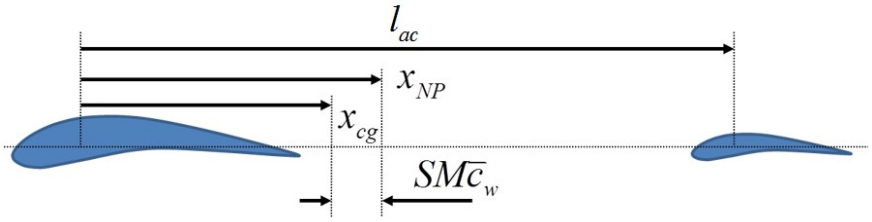

Fig. 2 Diagram of pitch trim.

$$\frac{l_{ac}}{c_w} = \frac{(1 + r_s r_{c_L})SM - \dfrac{C_{M_w}}{C_{L_w}} - r_s r_c \dfrac{C_{M_t}}{C_{L_w}}}{\dfrac{r_s\left(r_\alpha - r_{C_L}\right)}{1 + r_s r_\alpha}} \tag{2}$$

B. Solution by Decoupling

From the initial sizing, all other parameters except r_α and l_{ac} can be determined. Eq. (2) means that l_{ac} is a function of r_α. But r_α depend on l_{ac} due to the effect of the trailing vortices from the wing on the tail. To solve this problem, first l_{ac} as a function of r_α is plotted in Fig. 3 using Eq. (2). And then by using a 3-D panel tool such as AVL [2], r_α can be obtained as a function of l_{ac}. The crossing of the two curve represents the solution of l_{ac} that satisfies all the conditions.

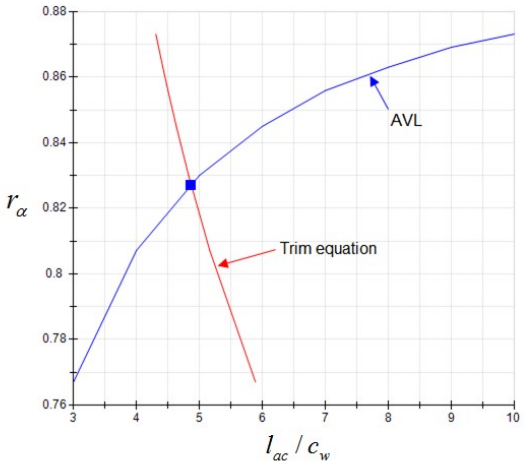

Fig. 3 Relation between the wing-tail distance and the lift curve slope ratio.

Once l_{ac} is determined, the relative incidence angle between the wing and tail is obtained by finding trim lift coefficients for wing and tail that match the preset values as shown in Fig. 4. In Fig. 4, trim C_Ls are plotted as a function of tail incidence angle while the incidence angle of the wing is fixed at zero. Note that trim trim angle of attack is also a function of the tail incidence angle.

An example solution set is summarized in Table 2 under the initial sizing parameters shown Table 1. DAE31 airfoil is used for the main wing and a modified DAE31 airfoil with a 70% reduction in camber is used for the tail. A short fuselage is achieved with a large static margin and tail volume coefficient. This methodology was used to design both the 2014 and 2015 HPAs.

Table 1 Initial sizing for verification

	Wing	Horizontal tail
Area [m^2]	20	5
C_L	1	0.5
Chord [m]	1	0.5
C_M	-0.15	-0.1
Static margin	15 %	

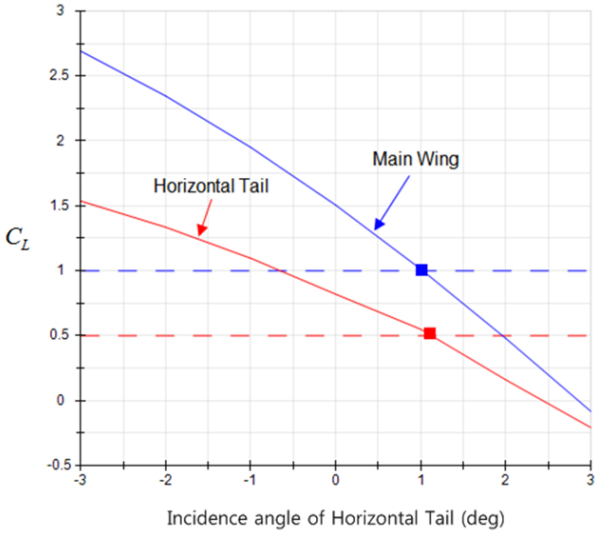

Fig. 4 Finding the relative incidence angle between wing and tail.

Table 2 Example solution by decoupling.

	Wing	Horizontal tail
C_L	1.08	0.55
Incidence angle [deg]	4.6	5.6
l_{ac} [m]	4.87	
x_{NP} [m]	1.08	
x_{cg} [m]	0.93	
Tail volume coefficient	1.05	

IV. Structural Design

Single CFRP tubular spar structure is used for the wings. Additional layers are attached to the top and bottom of the tubular spars to function as spar caps. Bracing wires are used to relieve the bending moment near the root. The chordwise location of the spar is at around 40% chord, which is near the center of pressure of the airfoil to minimize the torsional load on the spars. Coincidentally, for the DAE series airfoil used for the HPAs, the maximum thickness location is also close to the center of pressure. The structural design focuses on the layup pattern of the spar caps and the anchoring point of the bracing wire.

A. Layup Pattern Analysis

Due to the maximum length limit, spars are constructed in two pieces and the outer spar is inserted to the inner spar to form a single spar for half of the wing as shown in Fig. 5. The inner tapered tubular spar consists of one layer of ±45° fabric in the innermost layer to provide torsional rigidity and to prevent the subsequent unidirectional layers from splitting. The second layer is unidirectional. Spar caps cover the top and bottom 44° portion of the tube as shown in Fig. 5. The length of each unidirectional spar cap layer is calculated such that the maximum normal stress is below a limit. Because the outer spar needs to maintain a circular shape for bonding, the unidirectional spar caps cover the whole circumference of the spar. However, the weight penalty is minimal due to small spar diameters and smaller bending moments.

Assuming an elliptic lift distribution, $l(y)$, the bending moment is calculated using Eq. (3). From the bending moment, maximum normal stress is calculated using Eq. (4). The section moment of inertia, $I(y)$ is obtained using the layup patterns, and $r(y)$ is the radius of the tube at y. Note that when calculating $I(y)$, only the unidirectional layup is included. Each carbon fiber layer is very thin compared to the inner diameter of the spar so that the thickness effect can be ignored.

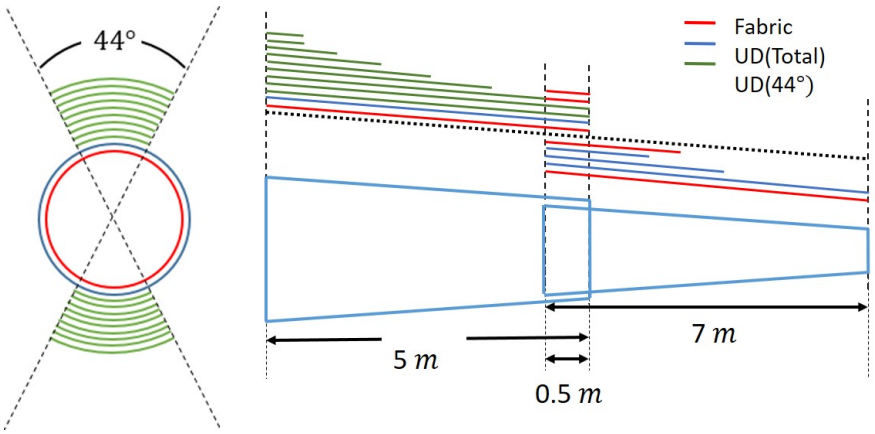

Fig. 5 Layer pattern of spar.

$$M(y) = \int_{y}^{b/2} (\hat{y} - y) l(\hat{y}) d\hat{y} \tag{3}$$

$$\tau_{max}(y) = \frac{M(y)}{I(y)} r(y) \tag{4}$$

Figure 6 shows the maximum normal stress as a function of the spanwise location. Maximum stress remains under 400 MPa, which assumes 2.5g condition with a maximum tensile strength of 1000 MPa.

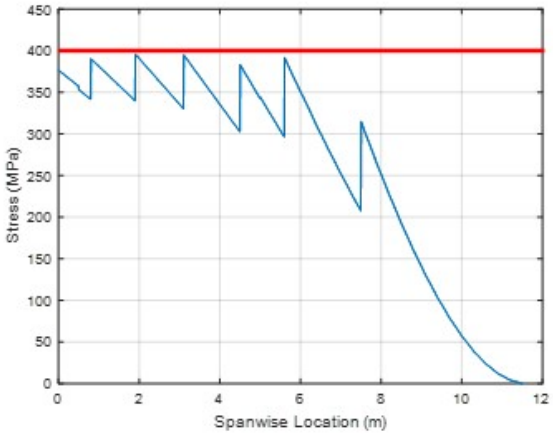

Fig. 6 Stress distribution.

B. Bracing Wire Position

Bracing wires are used to relieve the bending loads. It is necessary to find the optimal location of the wire along the wingspan. In this problem, structural deformation can be obtained from aerodynamic load and wire tension. However, the aerodynamic loads and, especially, the wire tension are again functions of the wing deformation. For the purpose of simplicity, the aerodynamic load is assumed to be fixed with an elliptic distribution, which is reasonable for high aspect ratio wings. The solution process is similar to the decoupling method used for the lifting tail design and is summarized in Fig. 7 [4].

As shown in Fig. 8 and Eq. (5), the wire tension is a function of the anchoring position along the wing, wing deformation, and the wire tension itself. T_{w_1} is the input tension of the bracing wire. Y_w is the anchoring position along the wing, and Z_w is the fixed vertical attachment position of the wire at the fuselage. T_{w_2} is the calculated output tension

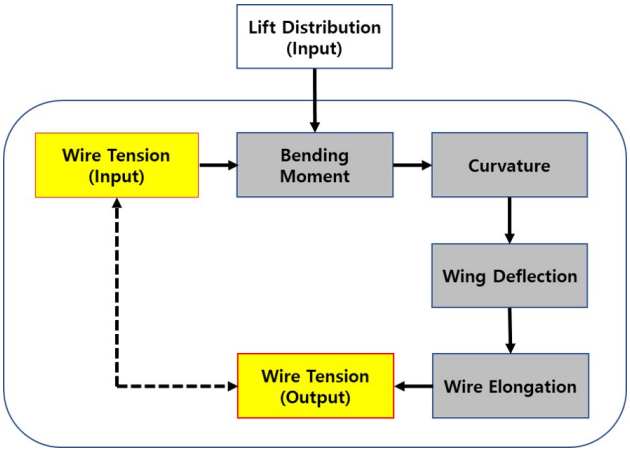

Fig. 7 Analysis process.

from the wire elongation and stiffness. If the input wire tension is small, it causes large wing deformation that results in a large output wire tension. Consequently, by gradually increasing the input wire tension, it is possible to find the solution as shown in Fig. 9 where the input and output tensions are the same.

$$T_{w_2} = f(y_w, z_w, T_{w_1}, l(y)) \tag{5}$$

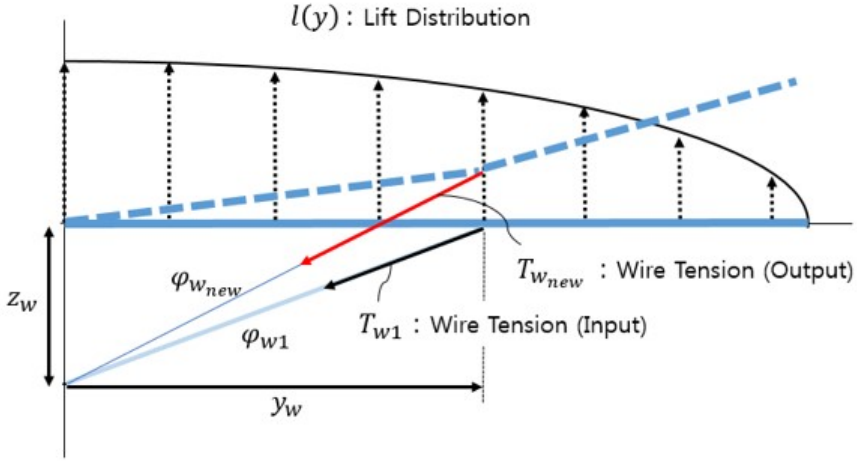

Fig. 8 Diagram for variable of wing deflection and elongation.

Since the length of spar is significantly larger than the diameter, simple Euler-Bernoulli beam model is used to calculate the wing deformation. By subtracting the bending moment caused by the wire, Eq. (3) becomes Eq. (6). The wing deformation is calculated by integrating the beam equation shown in Eq. (8).

$$M(y) = \begin{cases} \int_y^{b/2} (\hat{y} - y) l(\hat{y}) d\hat{y} - (y_w - y)(T_w \sin\theta) & (y \le y_w) \\ \int_y^{b/2} (\hat{y} - y) l(\hat{y}) d\hat{y} & (y_w < y) \end{cases} \tag{6}$$

where

$$\tan\theta = \frac{z_w}{y_w} \tag{7}$$

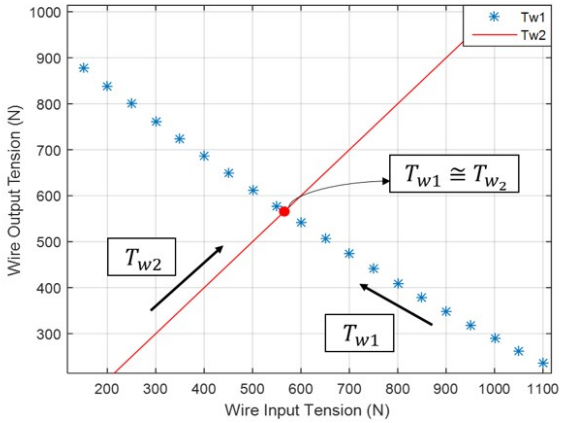

Fig. 9 Finding balanced bracing wire tension.

$$M(y) = -EI(y)\frac{d^2w}{dy^2} \tag{8}$$

Finally, using this method, it is possible to investigate the impact of changing the wire anchoring location, y_w. Figure 10 shows the wing tip deflection with respect to y_w. For determining the optimal wire location, it is necessary to consider the additional drag and weight of the wire. However, for the current study, only the maximum tip deflection is used for the constraint, and a minimum six meters is required to satisfy the given one meter tip deflection limit. For the 2015 HPA, six meters is used to minimize the length and weight of the wire. Note that in the previous section, spar cap layup is determined without considering the wire to satisfy the maximum stress constraints. So, wires provide an additional safety factor.

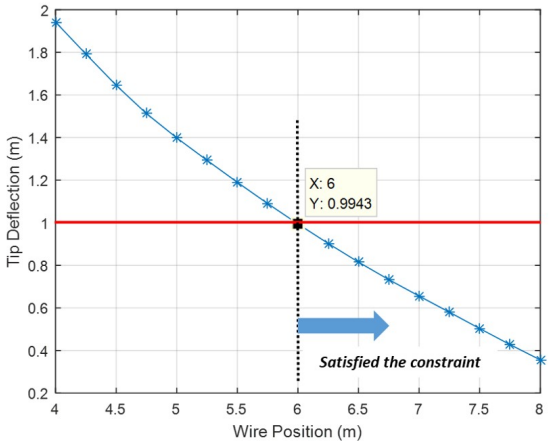

Fig. 10 Wire position region that satisfy requirement about the wing tip deflection

V. Aircraft Construction

The final specification of the 2014 and 2015 HPAs are shown in Tables 3 and 4, respectively. Main wing C_L was determined to be around 1.1 so that the root 2-D C_l is slightly below the maximum C_l of the DAE31 airfoil at the design Reynolds number. With the same transportation limitation, the span of the 2015 HPA was increased by 2 meters by making the wing four pieces. The span of the inner wing was slightly reduced from the 2014 aircraft, but two 1.5 m tips are added to increase the span and reduce induced drag. Since the outer section did not generate much lift, it was not

necessary to reinforce the joints for the additional wing pieces. Even with the larger main wing and also larger tail, the 2015 HPA was about 5 kg lighter than the 2014 aircraft, mainly due to optimized spar layup. Other weight-saving measures include CFRP V-brackets for the all-moving horizontal and vertical tails, replaced from the aluminum bracket as shown in Fig. 11.

Fig. 11 Bracket for tails (Left: aluminum construction for 2014 HPA, Right: CFRP construction for 2015 HPA)

After calculating the required tension of the bracing wire, 3 mm Dyneema rope was used for the bracing instead of steel wire, which was lighter and much easier to handle. Since the ropes were braided, to remove any slack, they were pre-stretched.

Ribs were laser cut out of commonly used foam boards and reinforced with balsa wood. Industrial strength double-sided tape was used to cover the wing with a polyester film. The tape was able to keep the film attached especially at the concave surface near the trailing edge of the lower side. Leading edge and trailing edges were constructed using hot wire cut foam blocks.

Both the horizontal and vertical tails are all moving design, actuated by two 1/4 scale RC servos. With the RC receiver and battery all located near the tails, the pilot used the modified RC transmitter to control the aircraft. So it was an uncommon fly-by-wireless setup but turned out to be effective.

Table 3 The geometry and aerodynamic specification of aircraft in 2014.

	Wing	Horizontal tail
Total span [m]	21	6
Constant span [deg]	12	
Root chord [m]	1.16	0.76
Tip chord [m]	0.71	
Aspect ratio	19.745	7.895
Area [m^2]	22.335	4.56
$C_{L_{tot}}$	1.117	
$C_{D_{induced}}$	0.020	

VI. Lessons Learned

As shown in Fig. 12, the 2014 HPA flew a couple of times during the competition with the maximum flight distance of around 75 meters. For the initial test, the aircraft had pitch up tendency, and the pilot was not able to correct it even with the full down elevator input. It was properly trimmed only after manually adjusting the incidence angle of the tail. Since the pilots do not have actual piloting experiences, it was difficult for them to pedal as hard as possible while trying to trim the aircraft. So, for the 2015 aircraft, initial trimming was performed by an external pilot. Due to the fly-by-wireless system, it was easy for an experienced RC pilot to hold the RC transmitter and adjust the pitch trim while the HPA pilot concentrated only on the pedaling.

Table 4 The geometry and aerodynamic specification of aircraft in 2015.

	Wing	Horizontal tail
Total span [m]	23	8.3
Constant span [deg]	6	
Root chord [m]	1.16	0.75
Tip chord [m]	0.71	
Aspect ratio	21.855	11.067
Area [m^2]	24.205	6.225
C_{L_w}	1.0224	-
C_{L_t}	-	0.5254
$C_{L_{tot}}$	1.1575	
$C_{D_{induced}}$	0.020	

Fig. 12 The moment of flight the 2014 HPA.

The most serious problem was the spar failure of the 2015 HPA. Figure 13 shows the 2015 HPA flying rather effortlessly with a moderate headwind. As can be seen from the picture, the wing deformation is also kept small and wing tip deflection seems to be within the design specification of one meter. Figure 14 shows the moment of failure when the left wing snapped right outside the wire anchoring point.

Fig. 13 2015 HPA before failure.

Fig. 14 2015 HPA moment of failure.

Later analysis revealed the stress distribution shown in Fig. 15. The failure location was exactly at the maximum stress location. As can be seen from Fig. 15, this maximum value exceeds the initial limit of 400 MPa. It was discovered that due to many design revisions, the ordered parts were not the optimized design shown in Fig. 6. Also, the wire can only relieve the load in between the two wire anchoring positions. However, judging from the small wing deflection, the stiffness appeared to be enough and the right wing did not display any weakness. Since the maximum stress was still under the tensile strength of 1000 MPa for the given carbon fiber, manufacturing defects are also suspected. In the end, one more unidirectional layer at the out spar could have prevented the failure, and it would have cost less than one kg of additional weight. A valuable lesson was learned about balancing aggressive design and leaving room for safety.

After the repair, the 2015 aircraft flew again. While cruising, both the wing tip, which are supposed to stay up, suddenly dropped, which caused the aircraft to stop flying. It was due to the slight washout aggravated by the repair process. Even though washout generally helps regular aircraft by preventing tip stall, for very flexible wings, it appears to be better to have a slight washin so that the wing tips stay up and maintain the U-shape of the wing. The wing deformation not only provides roll stability but also reduces induced drag by making the trailing vortices non-planar. Also it might be better to move the spar slightly backward so that the natural aerodynamic moment acts in the nose-up direction.

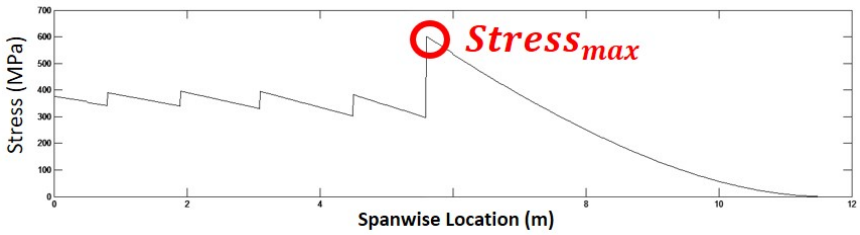

Fig. 15 The stress distribution at spar.

VII. Conclusions

The students in the Department of Aerospace Engineering, Inha University in the Republic of Korea built two HPAs during 2014 and 2015. With several aircraft design techniques developed for the HPAs, the two aircraft flew successfully with some glitches. Many valuable lessons were learned through the activities.

HPAs represent an interesting aircraft design problem. It is not as easy as making an RC aircraft to fly, where most of the issues can be addressed by increasing the power. However, it requires careful analysis of all the major disciplines, aerodynamics, structures, and control. Especially, most of the analysis can be performed using undergraduate level knowledge. Many of the students who participated in the competition continued their study in graduate school, which shows that the activity was very effective in motivating the students. The biggest hurdle is the logistics, due to the sheer size of the aircraft, which even changes the design of the aircraft. A middle ground competition such as designing and building an RC aircraft to carry a certain payload with a given power train might provide an opportunity for a similar level of analysis and design effort without the logistics problem.

Acknowledgments

The authors would like to thank Mr. Alec Proudfoot. He provided valuable guidance and tips regarding design and, especially, construction. The project was partly funded by Inha University.

References

[1] S, L. J., *The Feasibility of a Human-Powered Flight Between Creta and the Mainland of Greece*, Messachusetts Institute of Technology and Smithsonian Institution, 1986.

[2] Drela, M., and Youngren, H., *AVL 3.26 User Primer*, Messachusetts Institute of Technology, Cambridge, 2006.

[3] Park, B. S., and Lee, H. T., "Aircraft Conceptual Design Techniques to Assign Lift Coefficient Separately to Main Wing and Horizontal Tail," *KSAS Conference Journal*, 2014, pp. 899, 902.

[4] Kwon, K. J., Park, B. S., Kang, S. Y., and Lee, H. T., "Techniques to Analyze Bracing Wires in Humman Powered Aircraft," *KSAS Conference Journal*, 2016, pp. 678, 680.